Bioconjugate Chemistry

Article

pubs.acs.org/bc

Reduction-Sensitive Dual Functional Nanomicelles for Improved Delivery of Paclitaxel

Xiaolan Zhang,[†,‡,§] Ke Liu,[†,‡] Yixian Huang,[†,‡,§] Jieni Xu,[†,‡,§] Jiang Li,[†,‡,§] Xiaochao Ma,[†,‡] and Song Li*[,†,‡,§]

[†]Center for Pharmacogenetics, [‡]Department of Pharmaceutical Sciences, School of Pharmacy; [§]University of Pittsburgh Cancer Institute, University of Pittsburgh, Pittsburgh, Pennsylvania 15261, United States

Supporting Information

ABSTRACT: We have developed a dual-functional nanocarrier composed of a hydrophilic polyethylene glycol (PEG) and a hydrophobic farnesylthiosalicylate (FTS, a nontoxic Ras antagonist), which is effective in delivery of hydrophobic anticancer drug, paclitaxel (PTX). To facilitate the retention of the therapeutic activity of the carrier, FTS was coupled to PEG via a reduction-sensitive disulfide linkage (PEG_{5k}-S-S-FTS_2). PEG_{5k}-S-S-FTS_2 conjugate formed uniform micelles with very small size (~30 nm) and the hydrophobic drug PTX could be readily incorporated into the micelles. Interestingly, inclusion of a disulfide linkage into the PEG_{5k}-FTS_2 micellar system resulted in a 4-fold decrease in the critical micelle concentration (CMC). In addition, the PTX loading capacity and colloidal stability of PTX-loaded micelles were improved. HPLC-MS showed that parent FTS could be more effectively released from PEG_{5k}-S-S-FTS_2 conjugate in tumor cells/tissues compared to PEG_{5k}-FTS_2 conjugate *in vitro* and *in vivo*. PEG_{5k}-S-S-FTS_2 exhibited a higher level of cytotoxicity toward tumor cells than PEG_{5k}-FTS_2 without a disulfide linkage. Furthermore, PTX-loaded PEG_{5k}-S-S-FTS_2 micelles were more effective in inhibiting the proliferation of cultured tumor cells compared to Taxol and PTX loaded in PEG_{5k}-FTS_2 micelles. More importantly, PTX-loaded PEG_{5k}-S-S-FTS_2 micelles demonstrated superior antitumor activity compared to Taxol and PTX formulated in PEG_{5k}-FTS_2 micelles in an aggressive murine breast cancer model (4T1.2).

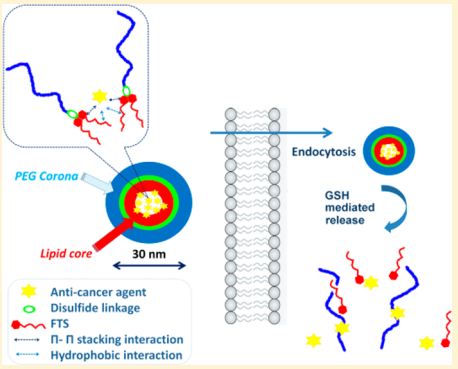

INTRODUCTION

Polymeric micelles are an attractive delivery system due to easy preparation, small size (10−100 nm), and the ability to solubilize hydrophobic drugs and accumulate preferentially within tumors.[1−5] We previously developed a nanocarrier based on polyethylene glycol (PEG)-derivatized farnesylthiosalicylate (FTS).[6] PEG_{5k}-FTS_2 readily formed micelles (20−30 nm) that were highly efficient in loading hydrophobic anticancer drugs such as paclitaxel (PTX).[6] More importantly, PTX-loaded PEG_{5k}-FTS_2 micelles achieved enhanced antitumor efficacy compared to Taxol formulation *in vivo*.[6] Different from most of the existing drug carriers that lack therapeutic effect, PEG_{5k}-FTS_2 itself exhibits antitumor activity.[6] FTS is a potent and especially nontoxic Ras antagonist.[7,8] Ras gene mutations can be found in one-third of human cancers, with the highest incidence in adenocarcinomas of the pancreas (90%), colon (50%), and lung (30%) tumors.[9] FTS can effectively inhibit the growth of many different types of tumors via inhibition of Ras-dependent signaling involved in tumor maintenance and progression.[10] The mechanism involves the dislodgement of Ras from the cell membrane and subsequent degradation of the protein.[11,12]

As a dual function carrier, the cleavability of the linkage between PEG and FTS in PEG_{5k}-FTS_2 conjugate is critical for its biological activity. In our previous study, we compared the antitumor activity of a conjugate with a labile ester linkage, PEG_{5K}-FTS_2(L), with that of a similar conjugate with a relatively stable amide linkage, PEG_{5K}-FTS_2(S).[6] PEG_{5K}-FTS_2(L) alone showed a significantly higher level of cytotoxicity toward tumor cells compared to PEG_{5K}-FTS_2(S), presumably due to a more ready release of FTS from PEG_{5K}-FTS_2(L) inside tumor cells.[6] In addition, delivery of PTX via PEG_{5K}-FTS_2(L) micelles led to an improved antitumor activity *in vivo* over PTX formulated in PEG_{5K}-FTS_2(S) micelles.[6]

In this study, we propose to incorporate into PEG_{5K}-FTS_2(L) an additional cleavable linkage (disulfide bond) to further facilitate the release of FTS following intracellular delivery to tumor cells. We choose the disulfide linkage because tumor cells have significantly higher concentrations of glutathione (GSH) than those in the extracellular fluids and the disulfide linkage has been widely used to develop a reduction-sensitive delivery system to facilitate drug release at the tumor site.[13−24] Our data showed that incorporation into PEG_{5K}-FTS_2(L) of a disulfide linkage led to an enhanced release of FTS inside tumor cells, which was associated with an improved cytotoxicity against tumor cells. Interestingly, the conjugate with a disulfide

Received: July 3, 2014
Revised: August 6, 2014
Published: August 8, 2014

   dx.doi.org/10.1021/bc500292j | *Bioconjugate Chem.* 2014, 25, 1689−1696

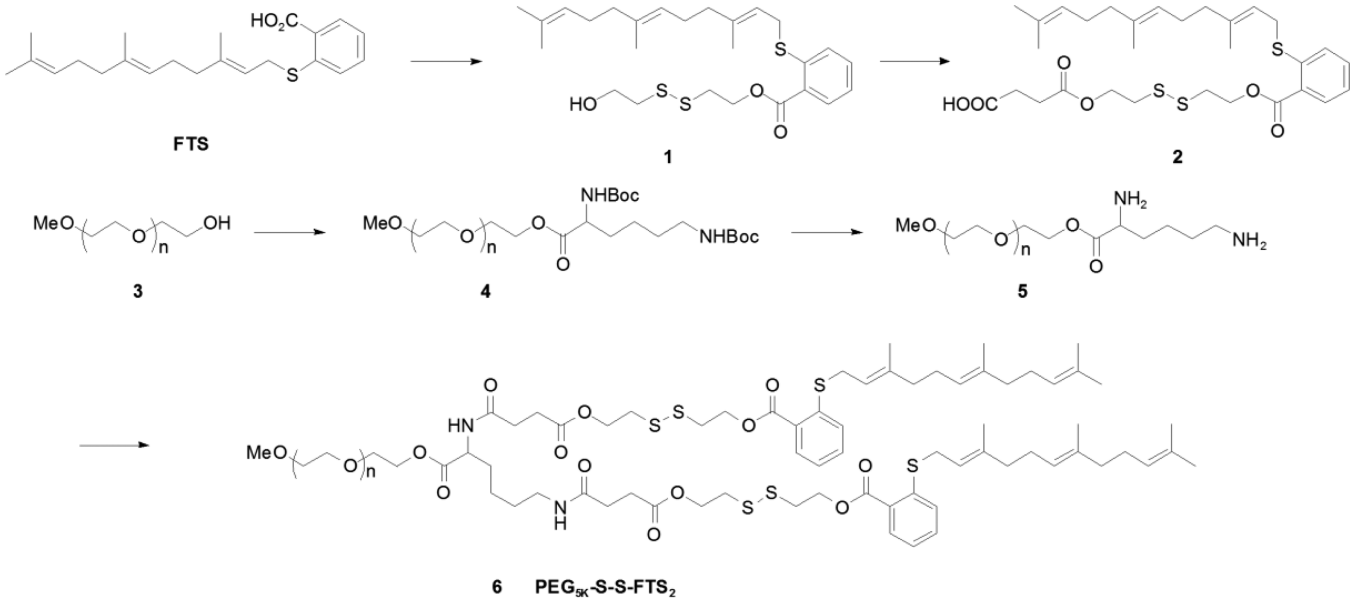

Figure 1. Synthesis scheme of PEG_{5k}-S-S-FTS_2 conjugate.

linkage (PEG_{5k}-S-S-FTS_2) exhibited a reduced critical micelle concentration (CMC) in addition to improved drug loading capacity and formulation stability. Finally, paclitaxel (PTX) formulated in PEG_{5k}-S-S-FTS_2 micelles was significantly more effective than the PEG_{5K}-FTS_2(L) formulation in inhibiting the tumor growth in a murine breast cancer model (4T1.2).

RESULTS

Synthesis of PEG_{5K}-S-S-FTS_2 Conjugate. To facilitate the retention of the antitumor activity of FTS, a cleavable disulfide linkage was used to couple FTS to a hydrophilic PEG (PEG_{5K}-S-S-FTS_2). The chemical structure of PEG_{5K}-S-S-FTS_2 is shown in Figure 1. As shown in ^{1}H NMR spectra (Supporting Information Figure S1), the signals at 3.63 ppm and 7−8 ppm were attributed to the methylene protons located at the terminus of PEG and the benzene ring protons of FTS, respectively. Additionally, the chemical shift of -CH_2-S-S-CH_2- (2.9−3.1 ppm) could be observed, which confirmed the presence of a disulfide linkage (Supporting Information Figure S1). The molecular weight of PEG_{5K}-S-S-FTS_2 was determined by MALDI-TOF mass spectrometry (Supporting Information Figure S2), which is close to the theoretical value of PEG_{5K}-S-S-FTS_2. Both ^{1}H NMR and MALDI-TOF mass spectra indicated the successful synthesis of PEG_{5K}-S-S-FTS_2 conjugate.

Characterization of PTX-Free and PTX-Loaded PEG_{5K}-S-S-FTS_2 Micelles. PEG_{5K}-S-S-FTS_2 was soluble in aqueous solution and readily self-assembled to form micelles with size around 30 nm (Figure 2A). Figure 2C shows the TEM images of PEG_{5K}-S-S-FTS_2 micelles. Spherical particles of uniform size were observed and the sizes of the particles observed under TEM were consistent with those measured by DLS. Figure 3 shows the CMCs of PEG_{5K}-FTS_2 and PEG_{5K}-S-S-FTS_2 micelles using pyrene as a fluorescence probe. It is interesting to note that incorporation into PEG_{5K}-FTS_2 of a disulfide linkage led to a ∼4-fold decrease in CMC. PTX can be readily loaded into PEG_{5K}-S-S-FTS_2 micelles. The spherical shape and size of the micelles were well retained following incorporation of PTX (Figure 2B,D). We then evaluated the loading capacity and stability of PTX-loaded PEG_{5K}-S-S-FTS_2 micelles and compared to those of PEG_{5K}-FTS_2 formulation. As shown in Table 1, PTX could be loaded in PEG_{5K}-S-S-FTS_2 micelles at a carrier/drug molar ratio as low as 1/1. In contrast, a minimal carrier/drug molar ratio of 2.5/1 was needed to formulate PTX in PEG_{5K}-FTS_2 micelles. Increasing the carrier/drug molar ratio was associated with an improvement in both drug loading efficiency (DLE) and the colloidal stability of PTX-loaded micelles (Table 1). In addition, PTX-loaded PEG_{5K}-S-S-FTS_2 micelles showed better colloidal stability than PEG_{5K}-FTS_2 formulation at all carrier/drug ratios examined (Table 1).

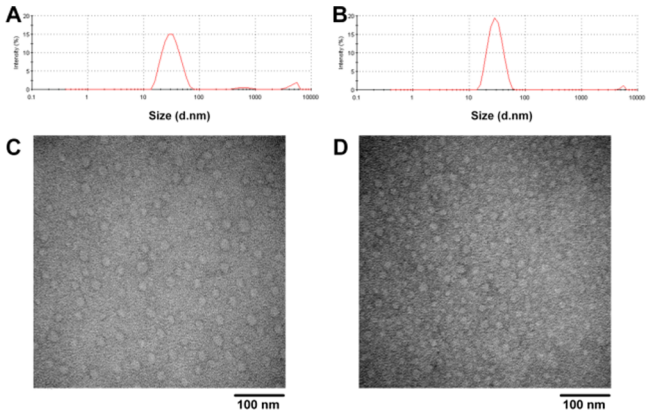

Figure 2. Particle size distribution of PTX-free PEG_{5K}-S-S-FTS_2 (A), and PTX-loaded PEG_{5K}-S-S-FTS_2 micelles (B). TEM images of PTX-free PEG_{5K}-S-S-FTS_2 (C), and PTX-loaded PEG_{5K}-S-S-FTS_2 micelles (D).

***In Vitro* Cytotoxicity of Drug-Free Micelles.** The antitumor activities of two PTX-free micelles, PEG_{5K}-S-S-FTS_2 and PEG_{5K}-FTS_2, were tested in HCT-116 and DU-145 cancer cell lines and compared to free FTS (Figure 4). PEG_{5K}-FTS_2 conjugate with an ester linkage was used as a reduction-insensitive control. As shown in Figure 4A, free FTS inhibited the HCT-116 cell growth in a concentration-dependent manner. PEG_{5K}-FTS_2 with a reduction-insensitive ester linkage was less active than free FTS in cytotoxicity (Figure 4A). Interestingly, incorporation into PEG_{5K}-FTS_2 of an additional disulfide linkage led to a significant improvement in cytotoxicity

dx.doi.org/10.1021/bc500292j | *Bioconjugate Chem.* 2014, 25, 1689−1696

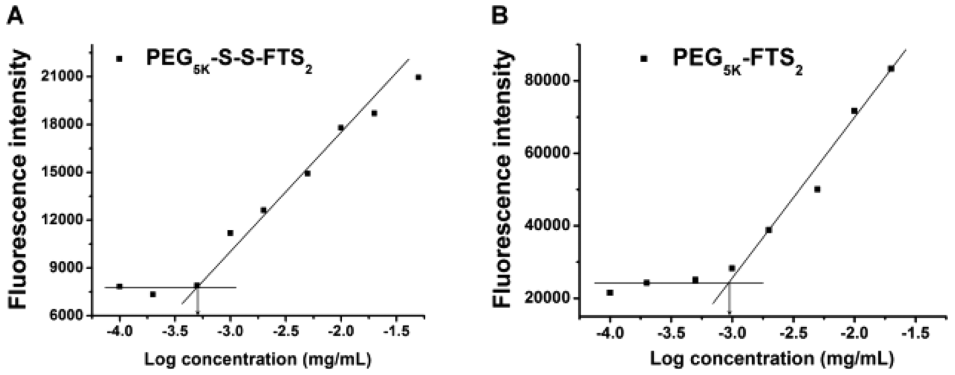

Figure 3. Critical micelle concentration (CMC) of PEG_{5K}-S-S-FTS_2 (A) and PEG_{5K}-FTS_2 (B) micelles.

Table 1. Physicochemical Characterization of Free Drug and PTX-Loaded PEG_{5k}-FTS_2 and PEG_{5k}-S-S-FTS_2 Micelles

micelles	molar ratio	conc. of PTX[a] (mg/mL)	size[b] (nm)	PDI[c]	DLC[d] (%)	DLE[e] (%)	stability[f] (h)
PEG_{5K}-FTS_2	-	-	17.6	0.20	-	-	-
PEG_{5K}-FTS_2:PTX	2.5:1	1	24.9	0.35	5.5	81.2	2
PEG_{5K}-FTS_2:PTX	5:1	1	25.6	0.23	2.8	97.6	20
PEG_{5K}-S-S-FTS_2	-	-	32.4	0.21	-	-	-
PEG_{5K}-S-S-FTS_2:PTX	1:1	1	28.5	0.22	12	85.2	1
PEG_{5K}-S-S-FTS_2:PTX	2.5:1	1	32.0	0.30	5.2	89.7	3.5
PEG_{5K}-S-S-FTS_2:PTX	5:1	1	30.2	0.35	2.6	94.8	30

[a]PTX concentration in micelle was kept at 1 mg/mL. Blank micelle concentration was 20 mg/mL. Values reported are the mean ± SD for triplicate samples. [b]Measured by dynamic light scattering particle sizer. [c]PDI = polydispersity index. [d]DLC = drug loading capacity. [e]DLE = drug loading efficiency. [f]Data means there was no noticeable size change during the follow-up period.

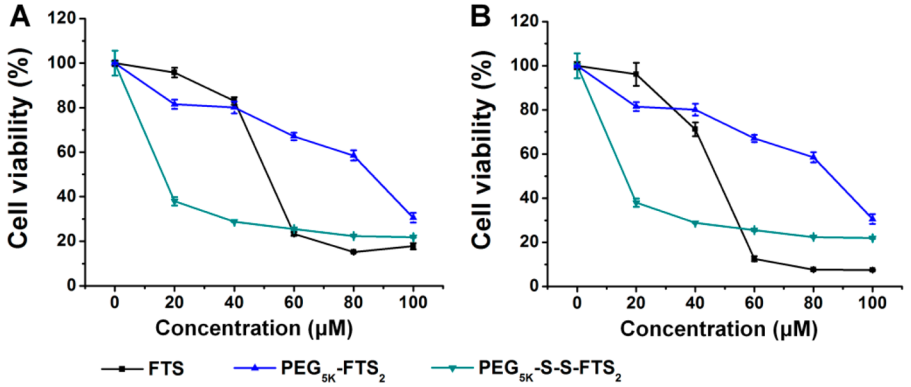

Figure 4. Cytotoxicity of drug free PEG_{5k}-FTS_2 and PEG_{5K}-S-S-FTS_2 micelles in comparison to free FTS in HCT-116 human colon carcinoma cell line (A) and DU-145 human prostate cancer cell line (B). Cells were treated for 72 h and cytotoxicity was determined by MTT assay.

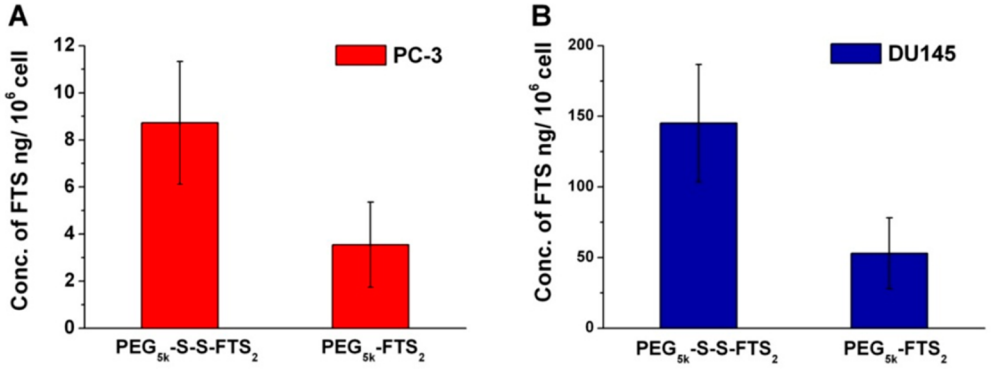

Figure 5. HPLC analysis of the amounts of released free FTS in PC-3 or DU-145 prostate cancer cells 72 h following treatment with PEG_{5K}-S-S-FTS_2 or PEG_{5K}-FTS_2 at a FTS concentration of 20 μM.

dx.doi.org/10.1021/bc500292j | *Bioconjugate Chem.* 2014, 25, 1689−1696

compared to both free FTS and PEG_{5K}-FTS_2 (Figure 4A). A similar result was observed in DU-145 cell line (Figure 4B).

Release of FTS from the PEG_{5K}-S-S-FTS_2 and PEG_{5K}-FTS_2 Conjugates. To investigate whether the improved cytotoxicity of PEG_{5K}-S-S-FTS_2 over PEG_{5K}-FTS_2 is attributed to a more effective release of FTS, HPLC-MS was employed to analyze FTS release inside PC-3 or DU-145 human prostate cancer cells 72 h following treatment with PEG_{5K}-FTS_2 or PEG_{5K}-S-S-FTS_2 micelles. We focused on the detection of the signal of parent FTS. The FTS extraction protocol had minimal impact on the integrity of PEG_{5K}-S-S-FTS_2 as demonstrated in a preliminary study (data not shown). Figure 5A shows that incorporation into PEG_{5K}-FTS_2 a disulfide linkage led to a 2- to 3-fold increase in the amounts of free FTS detected in PC-3 cells (Figure 5A). A similar result was observed in DU-145 cell line (Figure 5B). We also conducted a preliminary study on the release of FTS in tumor tissues *in vivo*. Female BALB/c mice bearing 4T1.2 tumor (~1 cm) received i.v. injection of PEG_{5K}-S-S-FTS_2 and PEG_{5K}-FTS_2 micelles at the same dose and the amounts of free FTS in the tumor tissues were examined 24 h later. As shown in Figure 6, a strong signal of FTS was detected

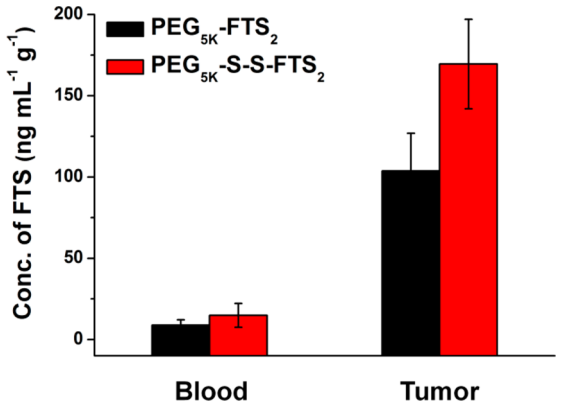

Figure 6. HPLC-MS analysis of FTS in blood and tumors 24 h following i.v. administration of PEG_{5K}-FTS_2 and PEG_{5K}-S-S-FTS_2.

in the tumor tissues while very little FTS signal was found in the blood. It is also apparent that significantly greater amounts of free FTS were found in the tumors treated with PEG_{5K}-S-S-FTS_2 compared to the PEG_{5K}-FTS_2-treated tumors (Figure 6), indicating that FTS is more readily cleaved from PEG_{5K}-S-S-FTS_2 micelles at the tumor sites.

***In Vitro* Cytotoxicity of Drug-Loaded Micelles.** Figure 7 shows the *in vitro* cytotoxicity of PTX formulated in PEG_{5K}-FTS_2 or PEG_{5K}-S-S-FTS_2 micelles, in comparison with Taxol formulation in MCF-7 and HCT-116 cells. Taxol inhibited the proliferation of MCF-7 breast cancer cells in a concentration dependent manner (Figure 7A). Delivery of PTX via PEG_{5K}-FTS_2 micelles led to a slight increase in cytotoxicity against MCF-7 tumor cells. More importantly, PTX formulated in PEG_{5K}-S-S-FTS_2 micelles were more active than both Taxol formulation and PTX-loaded PEG_{5K}-FTS_2 micelles in inhibiting the tumor cell growth, particularly at low PTX concentrations (Figure 7A). A similar result was observed in a colon carcinoma cell line, HCT-116 (Figure 7B).

***In Vivo* Therapeutic Study.** Figure 8 shows the *in vivo* therapeutic activity of PTX formulated in PEG_{5K}-S-S-FTS in an aggressive murine breast cancer model (4T1.2). PEG_{5K}-S-S-FTS_2 micelles alone showed no effects in inhibiting the tumor growth at the concentration used. This is due to a relatively low concentration of FTS in this group. Taxol formulation showed a modest tumor growth inhibition at a dose of 10 mg PTX/kg (Figure 8A). In contrast, both PTX-loaded PEG_{5K}-FTS_2 and PEG_{5K}-S-S-FTS_2 micelles were more effective than Taxol formulation at the same dose (Figure 8A). More importantly, PTX formulated in PEG_{5K}-S-S-FTS_2 micelles exhibited even more potent tumor growth inhibition than PTX-loaded PEG_{5K}-FTS_2 micelles ($P < 0.05$) (Figure 8A). No significant changes in body weight were detected in all treatment groups compared to PBS control group (Figure 8B).

DISCUSSION

We have previously reported that PTX-loaded PEG_{5K}-FTS_2(L) micelles showed better antitumor activity than Taxol formulation, which could be ascribed to their preferential tumor accumulation and a possible synergistic effect between PEG_{5K}-FTS_2(L) carrier and loaded PTX.[6] In this study, we have shown that inclusion of a disulfide linkage led to a further improvement in the therapeutic activity compared to PTX formulated in PEG_{5k}-FTS_2(L) micelles and Taxol *in vivo* (Figure 8).

Similar to PEG_{5K}-FTS_2(L), PEG_{5K}-S-S-FTS_2 readily self-assembled to form micelles in aqueous solution with relatively

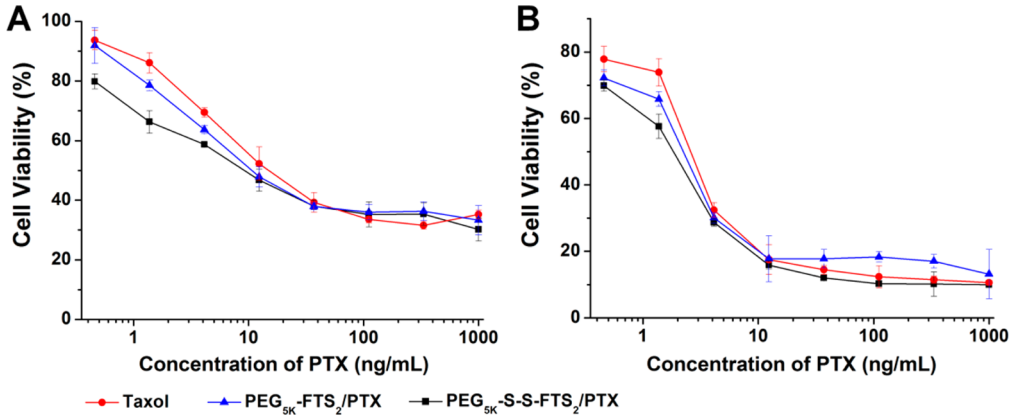

Figure 7. Cytotoxicity of PTX-loaded PEG_{5k}-FTS_2 and PEG_{5k}-S-S-FTS_2 micelles in comparison to Taxol formulation in MCF-7 human breast carcinoma cell line (A) and HCT-116 human colon carcinoma cell line (B). Cells were treated for 72 h and cytotoxicity was determined by MTT assay.

dx.doi.org/10.1021/bc500292j | *Bioconjugate Chem.* 2014, 25, 1689−1696

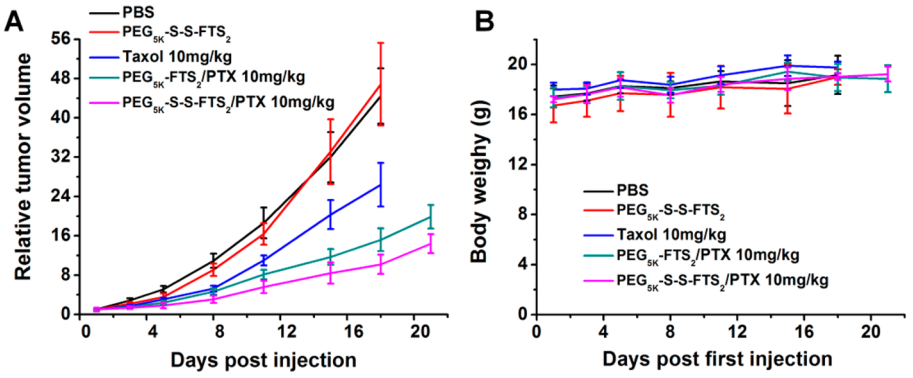

Figure 8. Antitumor activity of PTX formulated in PEG_{5K}-S-S-FTS_2 micelles in a syngeneic murine breast cancer model (4T1.2) (A). $P < 0.05$ (PTX/PEG_{5K}-S-S-FTS_2 vs PTX/PEG_{5K}-FTS_2). $N = 5$. Changes of body weight in mice receiving different treatments (B).

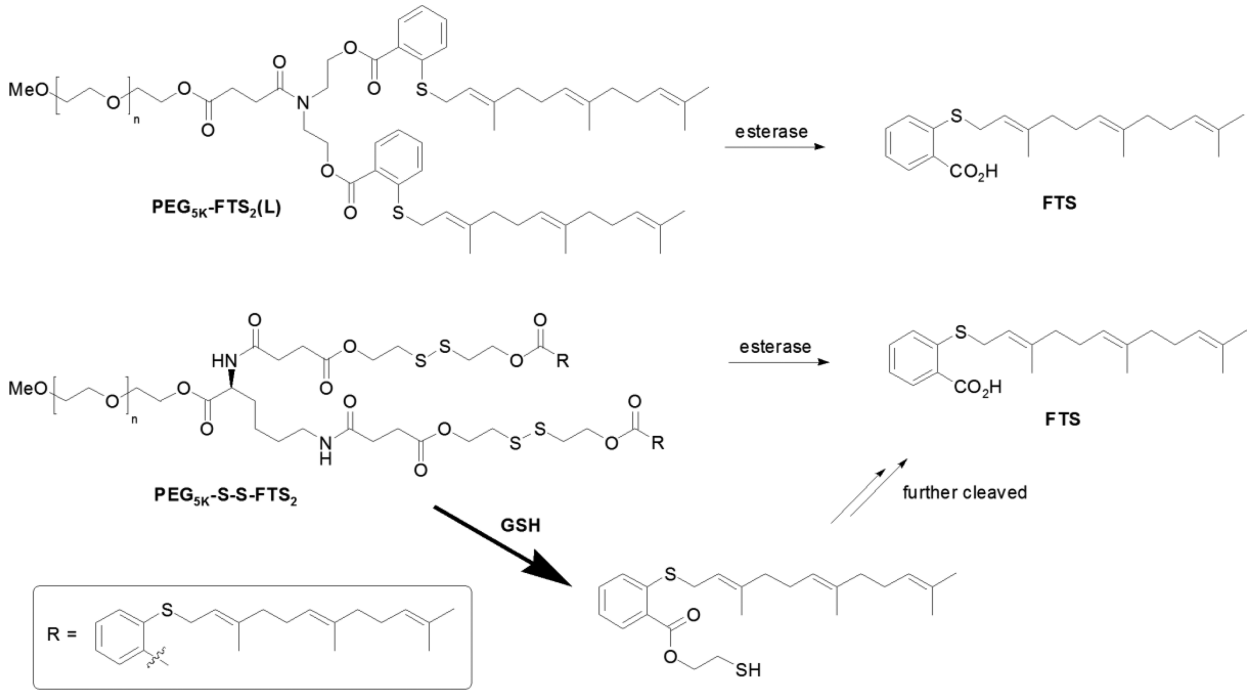

Figure 9. Proposed mechanism for the release of FTS from PEG_{5K}-FTS_2 and PEG_{5K}-S-S-FTS_2 conjugates following intracellular delivery to tumor cells.

small size (~30 nm) (Table 1). Such small size shall enable the carrier to be highly effective in passive accumulation at and deep penetration into solid tumors, including the poorly vascularized tumors.[1,25] Interestingly, inclusion of a disulfide linkage led to an improvement in both PTX loading capacity and the colloidal stability of PTX-loaded micelles (Table 1). We further noticed that incorporation into PEG_{5K}-FTS_2(L) a disulfide linkage resulted in a 4-fold decrease in CMC (Figure 3). A lower CMC will enable the micelles to be more stable in the blood circulation following systemic administration.[26] This is likely due to an improved cooperation in both carrier/carrier and carrier/drug interactions following incorporation of a flexible disulfide linkage into the lipid motif of the carrier. The increase in the chain length of lipid motif following inclusion of a disulfide linkage may also contribute to the improved PTX loading capacity and formulation stability.

HPLC-MS analysis showed that parent FTS can be detected from cultured cancer cells following treatment with PEG_{5K}-FTS_2(L) micelles (Figure 5), suggesting that FTS can be released from the conjugate via intracellular esterases. It is also apparent that significantly higher levels of parent FTS were found in tumor cells treated with PEG_{5K}-S-S-FTS_2 conjugate (Figure 5). A similar result was found in tumor tissues (Figure 6) in tumor-bearing mice receiving i.v. administration of PEG_{5K}-FTS_2(L) or PEG_{5K}-S-S-FTS_2 conjugate. FTS can be released from the PEG_{5K}-S-S-FTS_2 conjugate via two different mechanisms: one is direct cleavage of the ester linkage adjacent to FTS to generate the parent FTS, and the other involves reduction of the disulfide linkage first, followed by cleavage of the ester linkage to generate the parent FTS (Figure 9). The fact that significantly greater amounts of parent FTS were released from cells treated with PEG_{5K}-S-S-FTS_2 would suggest that the latter is the major mechanism for FTS release (Figure 9). This is probably because direct release of FTS from PEG_{5K}-FTS_2(L) by intracellular esterases is relatively ineffective due to the steric hindrance imposed by PEG. On the other hand, cleavage of disulfide linkage is a more effective process inside tumor cells due to the significantly increased GSH levels in tumor cells.[15,17] Once released from the conjugate, the small

dx.doi.org/10.1021/bc500292j | Bioconjugate Chem. 2014, 25, 1689−1696

molecule intermediate can be effectively hydrolyzed by the intracellular esterases to generate the parent FTS (Figure 9).

In vitro cytotoxicity showed that PEG_{5K}-S-S-FTS_2 conjugate was significantly more effective in inhibiting the proliferation of cultured tumor cells compared to PEG_{5K}-FTS_2(L) conjugate (Figure 4). The increased cytotoxicity of PEG_{5K}-S-S-FTS_2 is most likely due to a facilitated release of FTS following inclusion of an additional cleavable disulfide linkage. It is interesting to note that PEG_{5K}-SS-FTS_2 also exhibited higher levels of cytotoxicity than free FTS at low concentrations (Figure 4). This is unlikely due to the surfactant activity of the conjugate as PEG_{5K}-SS-FTS_2 showed minimal hemolytic activity at even much higher concentrations (data not shown). It is possible that PEG_{5K}-SS-FTS_2 is more effectively taken by tumor cells than free FTS, which will be further examined in the future. PEG_{5K}-S-S-FTS_2 not only retained the biological activity well, but also served as an efficient carrier to deliver hydrophobic drug PTX. PTX formulated in PEG_{5K}-S-S-FTS_2 micelles showed a level of cytotoxicity that was higher than that of either Taxol or PTX formulated in PEG_{5K}-FTS_2(L) micelles (Figure 7), particularly at low PTX concentrations.

In vivo antitumor study showed that PTX formulated in PEG_{5K}-FTS_2(L) micelles were significantly more effective than Taxol formulation in a syngeneic murine breast cancer model (Figure 8), which is consistent with our previous report.[6] It is also apparent that inclusion of a disulfide linkage in PEG_{5K}-FTS_2(L) micellar system led to a further improvement in antitumor activity (Figure 8). The improved performance is likely attributed to a more effective cleavage of FTS from the conjugate in the tumor tissue, which shall lead to not only enhanced intracellular delivery of FTS but also facilitated release of loaded drug following disassembly of micelles. It remains to be investigated whether the improved carrier/drug interaction and the reduced CMC of the PEG_{5K}-S-S-FTS_2 micellar system also contribute to the overall improvement in antitumor activity.

CONCLUSION

An improved dual-functional micellar carrier composed of a PEG shell and FTS core via a disulfide linkage (PEG_{5k}-S-S-FTS_2) was developed. PEG_{5K}-S-S-FTS_2 retained the FTS biological activity well, which was attributed to an effective release of FTS from the conjugate following intracellular delivery. In addition, PEG_{5K}-S-S-FTS_2 readily self-assembled into small-sized micelles and formed stable mixed micelles with PTX. More importantly, PTX-loaded PEG_{5K}-S-S-FTS_2 micelles demonstrated more effective therapeutic effects *in vivo* over Taxol formulation and PTX-loaded PEG_{5K}-FTS_2 micelles.

EXPERIMENTAL PROCEDURES

Materials. Paclitaxel (98%) was purchased from AK Scientific Inc. (CA, USA). FTS and PEG_{5K}-FTS_2 conjugate were synthesized according to published literature.[6,7] Poly(ethylene glycol) methyl ether (MeO-PEG-OH, MW = 5000 kDa), dimethyl sulfoxide (DMSO), succinate anhydride, diethanolamine, trypsin-EDTA solution, Dulbecco's Modified Eagle's Medium (DMEM), and 3-(4,5-dimethylthiazol-2-yl)-2,5-diphenyl tetrazolium bromide (MTT) were all purchased from Sigma-Aldrich (MO, USA). Di-Boc-lysine, triethylamine (TEA), and trifluoroacetic acid (TFA) were obtained from Acros Organic (NJ, USA). Bis(2-hydroxyethyl) disulfide, dicyclohexylcarbodiimide (DCC), and *N*-hydroxysuccinimide (NHS) were purchased from Alfa Aesar (MA, USA). 4-(Dimethylamino)pyridine (DMAP) was purchased from Calbiochem-Novabiochem Corporation (CA, USA). All solvents used in this study were HPLC grade.

Cell Culture. MCF-7 is a human breast carcinoma cell line. 4T1.2 is a mouse metastatic breast cancer cell line. HCT-116 is a human colon carcinoma cell line. PC-3 and DU-145 are human prostate cancer cell lines. All cell lines were cultured in DMEM containing 5% FBS and 1% penicillin−streptomycin at 37 °C in a humidified 5% CO_2 atmosphere.

Animals. Female BALB/c mice, 4−6 weeks in age, were purchased from Charles River (Davis, CA). All animals were housed under pathogen-free conditions according to AAALAC guidelines. All animal-related experiments were performed in full compliance with institutional guidelines and approved by the Animal Use and Care Administrative Advisory Committee at the University of Pittsburgh.

Synthesis of PEG_{5K}-S-S-FTS_2 Conjugate. Figure 1 shows the synthesis route of PEG_{5K}-S-S-FTS_2 conjugate. Synthesis and structural characterizations are detailed below.

Compound ***1***. Bis(2-hydroxyethyl) disulfide (1.54 g, 10 mmol) was added to a solution of FTS (3.58 g, 10 mmol), DCC (3.09 g, 15 mmol), and DMAP (122 mg, 1 mmol) in CH_2Cl_2 (50 mL). The mixture was stirred at room temperature until TLC showed completion of reaction. The mixture was filtered through cotton and the filtrate was concentrated on a rotary evaporator. The residue was chromatographed (1:4 EtOAc/PE) on silica gel to afford the compound **1** (3.2 g, 6.5 mmol, 65%). ^{1}H NMR (400 MHz, $CDCl_3$) δ 7.99−7.97 (m, 1H), 7.45−7.41 (m, 1H), 7.32−7.28 (m, 1H), 7.17−7.13 (m, 1H), 5.36−5.32 (m, 1H), 5.10−5.07 (m, 2H), 4.59 (t, J = 6.8 Hz, 2H), 3.88−3.87 (m, 2H), 3.58−3.56 (m, 2H), 3.06 (t, J = 6.8 Hz, 2H), 2.89 (t, J = 6 Hz, 2H), 2.09−1.97 (m, 8H), 1.73 (s, 3H), 1.68 (s, 3H), 1.60 (s, 6H).

Compound ***2***. Succinic anhydride (2 g, 20 mmol) was added to a solution of compound **1** (4.94 g, 10 mmol) and DMAP (2.44 g, 20 mmol) in $CHCl_3$ (50 mL), and the mixture was refluxed until TLC showed completion of reaction. The mixture was concentrated on a rotary evaporator and the residue was chromatographed (1:1 EtOAc/PE) on silica gel to afford the compound **2** (5.8 g, 6.5 mmol, 97%). ^{1}H NMR (400 MHz, $CDCl_3$) δ 7.99−7.97 (m, 1H), 7.41−7.38 (m, 1H), 7.29−7.27 (m, 1H), 7.14−7.10 (m, 1H), 5.30−5.27 (m, 1H), 5.06−5.03 (m, 2H), 4.54 (t, J = 6.8 Hz, 2H), 4.33 (t, J = 6.8 Hz, 2H), 3.55−3.53 (m, 2H), 3.03 (t, J = 6.4 Hz, 2H), 2.89 (t, J = 6.4 Hz, 2H), 2.62−2.61 (m, 4H), 2.04−1.92 (m, 8H), 1.69 (s, 3H), 1.64 (s, 3H), 1.55 (s, 6H).

Compound ***5***. Compound **5** was synthesized from compound **3** following a published method.[6]

Compound ***6***. DCC, DMAP, compound **2**, and compound **5** were dissolved in CH_2Cl_2 with a molar ratio of 1:6:3:0.3 and allowed to react overnight at room temperature. The solution was filtered and precipitated in diethyl ether and ethanol twice, respectively. Compound **6** was obtained by further drying under vacuum.

Preparation and Characterization of PTX-Loaded PEG_{5K}-S-S-FTS_2 Micelles. PTX-solubilized PEG_{5K}-S-S-FTS_2 micelles were prepared via a solvent evaporation method following our published protocol.[6,18] Briefly, PTX (10 mM in chloroform) and PEG_{5K}-S-S-FTS_2 conjugate (10 mM in chloroform) were mixed with various carrier/drug ratios. A film of drug/carrier mixture was formed by removed the organic solvent and the film was further dried under vacuum.

PTX-loaded micelles were formed by adding DPBS to hydrate the thin film followed by gentle vortexing. The PTX loading efficiency was measured by high performance liquid chromatography (HPLC) (Alliance 2695−2998 system) as described previously.[6] Drug loading capacity (DLC) and drug loading efficiency (DLE) were calculated according to the following equation:

$$\mathrm{DLC}(\%) = [\text{weight of drug used}/(\text{weight of polymer} + \text{drug used})] \times 100\%$$

$$\mathrm{DLE}(\%) = (\text{weight of loaded drug}/\text{weight of input drug}) \times 100\%$$

Morphology, micelle size, and size distribution were assessed by transmission electron microscopy (TEM) and dynamic light scattering (DLS) following our published protocol.[4] The critical micelle concentration (CMC) of PEG_{5K}-S-S-FTS_2 micelles was determined using pyrene as a fluorescence probe.[27]

Release of FTS from the PEG_{5K}-S-S-FTS_2 and PEG_{5K}-FTS_2 Conjugates. DU-145 and PC-3 cells were seeded in 6-well plates. After 24 h of incubation in DMEM with 5% FBS, the old medium was removed and the cells were incubated for 72 h in the presence of drug-free PEG_{5K}-S-S-FTS_2 or PEG_{5K}-FTS_2 micelles. The cells were washed with ice-cold PBS three times and solubilized via a mixture of MeOH and H_2O. The lysates were vortexed and then centrifuged at 14 000 rpm for 10 min at 4 °C. Supernatants were transferred to another set of 1.5 mL microtubes and stored at −80 °C for MS analysis. The amount of FTS in each sample was quantified by Waters' SYNAPT G2-S mass spectrometer according to the literature.[28,29] Chromatographic separation of FTS was performed on an Acquity UPLC BEH C18 column (2.1 × 50 mm, 1.7 μm, Waters). The mobile phase A (MPA) was 0.1% formic acid in acetonitrile, and mobile phase B was 0.1% formic acid in water. The flow rate of mobile phase was 0.40 mL/min and the column temperature was maintained at 50 °C. Data were processed using QuanLynx (v 4.1, Waters). Extracted ion chromatograms (EICs) were extracted using a 20 mDa window centered on the expected m/z 357.189 for FTS.

Similarly, FTS release was examined with tumor tissues from female BALB/c mice bearing 4T1.2 tumor (~1 cm). Groups of 4 mice received i.v. injection of PEG_{5K}-FTS_2 or PEG_{5K}-S-S-FTS_2 conjugate at a dose of 58.5 μmol/kg. One day post injection, blood and tumors were collected. Samples were homogenized with PBS, and then mixed with 2 volumes of acetonitrile. The mixture was vortexed for 1 min, incubated for 5 min, and centrifuged at 14 000 rpm for 10 min at 4 °C. The supernatants were decanted from each sample into a clean centrifugation tube for MS analysis and FTS was then analyzed as described above.

***In Vitro* Cytotoxicity Study.** The cytotoxicity of PTX formulated in PEG_{5K}-S-S-FTS_2 micelles was assessed with several cancer cell lines and compared to Taxol and PTX loaded in PEG_{5K}-FTS_2 micelles, respectively. Briefly, MCF-7 cells (5000 cells/well) and HCT-116 cells (1000 cells/well) were seeded in 96-well plates. After incubation in DMEM with 5% FBS and 1% streptomycin−penicillin for 24 h, the old medium was removed and the cells were further incubated for 3 days in the presence of indicated concentrations of PTX formulated in Cremophor/EL, PEG_{5K}-S-S-FTS_2, or PEG_{5K}-FTS_2 micelles. Cell viability was then assessed by MTT assay following our published literature.[6] Similarly, the cytotoxicity of drug-free PEG_{5K}-S-S-FTS_2 micelles was examined and compared to free FTS and PEG_{5K}-FTS_2 micelles as described above.

***In Vivo* Therapeutic Study.** An aggressive murine breast cancer model (4T1.2) was used to examine the *in vivo* therapeutic effect of different formulations of PTX. Tumors were induced by inoculation of 4T1.2 cells (1×10^5) in 100 μL PBS at the right flank of female BALB/c mice. After tumors in the mice reached a tumor volume of ~40 mm^3, treatments were started and this day was designated as day 1. On the first day, tumor (4T1.2)-bearing mice were randomly divided into five groups ($n = 5$) and administered i.v. with PBS (control), drug-free PEG_{5K}-S-S-FTS_2 micelles, Taxol (10 mg PTX/kg), PTX-loaded PEG_{5K}-FTS_2, and PEG_{5K}-S-S-FTS_2 micelles (10 mg PTX/kg), respectively, on days 1, 3, 6, 8, 10, and 12. Tumor sizes were measured twice a week and tumor volumes were calculated by the formula: $(L \times W^2)/2$, where L and W represent the longest and shortest in tumor diameters (mm). Each group was compared by relative tumor volume (RTV) (where RTV equals to the tumor volume divided by the initial tumor volume before treatment). The body weights of all mice from each group were measured twice a week.

Statistical Analysis. Data are presented as mean ± standard deviation (SD). Statistical analysis was performed by Student's t test for comparison of two groups, and comparisons for multiple groups were made with one-way analysis of variance (ANOVA), followed by Newman-Keuls test if the overall $P < 0.05$. In all statistical analysis, the threshold of significance was defined as $P < 0.05$.

■ ASSOCIATED CONTENT

Supporting Information

Additional figures as discussed in the text. This material is available free of charge via the Internet at http://pubs.acs.org.

■ AUTHOR INFORMATION

Corresponding Author

*Tel: 412-383-7976. Fax: 412-648-1664. E-mail: sol4@pitt.edu.

Notes

The authors declare no competing financial interest.

■ ACKNOWLEDGMENTS

This work was supported by NIH grants R01CA174305, R01GM102989, and R21CA173887. We would like to thank Drs. Donna Stolz and Ming Sun for their help with negative EM study. We would like to thank Dr. Raman Venkataramanan and Wenchen Zhao for their help with drug loading efficiency test.

■ REFERENCES

(1) Bourzac, K. (2012) Nanotechnology: Carrying drugs. *Nature 491*, S58−60.

(2) Torchilin, V. (2009) Multifunctional and stimuli-sensitive pharmaceutical nanocarriers. *Eur. J. Pharm. Biopharm. 71*, 431−444.

(3) Zhang, X., Huang, Y., and Li, S. (2014) Nanomicellar carriers for targeted delivery of anticancer agents. *Ther. Delivery 5*, 53−68.

(4) Zhang, P., Lu, J., Huang, Y., Zhao, W., Zhang, Y., Zhang, X., Li, J., Venkataramanan, R., Gao, X., and Li, S. (2014) Design and evaluation of a PEGylated lipopeptide equipped with drug-interactive motifs as an improved drug carrier. *AAPS J. 16*, 114−124.

(5) Lu, J., Huang, Y., Zhao, W., Marquez, R. T., Meng, X., Li, J., Gao, X., Venkataramanan, R., Wang, Z., and Li, S. (2013) PEG-derivatized

embelin as a nanomicellar carrier for delivery of paclitaxel to breast and prostate cancers. *Biomaterials 34*, 1591−1600.
(6) Zhang, X., Lu, J., Huang, Y., Zhao, W., Chen, Y., Li, J., Gao, X., Venkataramanan, R., Sun, M., Stolz, D. B., Zhang, L., and Li, S. (2013) PEG-farnesylthiosalicylate conjugate as a nanomicellar carrier for delivery of paclitaxel. *Bioconjugate Chem. 24*, 464−472.
(7) Marciano, D., Ben-Baruch, G., Marom, M., Egozi, Y., Haklai, R., and Kloog, Y. (1995) Farnesyl derivatives of rigid carboxylic acids-inhibitors of ras-dependent cell growth. *J. Med. Chem. 38*, 1267−1272.
(8) Haklai, R., Weisz, M. G., Elad, G., Paz, A., Marciano, D., Egozi, Y., Ben-Baruch, G., and Kloog, Y. (1998) Dislodgment and accelerated degradation of Ras. *Biochemistry 37*, 1306−1314.
(9) Bos, J. L. (1989) Ras oncogenes in human cancer: a review. *Cancer Res. 49*, 4682−4689.
(10) Goldberg, L., Haklai, R., Bauer, V., Heiss, A., and Kloog, Y. (2009) New derivatives of farnesylthiosalicylic acid (salirasib) for cancer treatment: farnesylthiosalicylamide inhibits tumor growth in nude mice models. *J. Med. Chem. 52*, 197−205.
(11) Paz, A., Haklai, R., Elad-Sfadia, G., Ballan, E., and Kloog, Y. (2001) Galectin-1 binds oncogenic H-Ras to mediate Ras membrane anchorage and cell transformation. *Oncogene 20*, 7486−7493.
(12) Rotblat, B., Ehrlich, M., Haklai, R., and Kloog, Y. (2008) The Ras inhibitor farnesylthiosalicylic acid (Salirasib) disrupts the spatiotemporal localization of active Ras: a potential treatment for cancer. *Methods Enzymol. 439*, 467−489.
(13) McCarley, R. L. (2012) Redox-responsive delivery systems. *Annu. Rev. Anal. Chem. 5*, 391−411.
(14) Saito, G., Swanson, J. A., and Lee, K. D. (2003) Drug delivery strategy utilizing conjugation via reversible disulfide linkages: role and site of cellular reducing activities. *Adv. Drug Delivery Rev. 55*, 199−215.
(15) Meng, F., Hennink, W. E., and Zhong, Z. (2009) Reduction-sensitive polymers and bioconjugates for biomedical applications. *Biomaterials 30*, 2180−2198.
(16) Huang, H., Zhang, X., Yu, J., Zeng, J., Chang, P. R., Xu, H., and Huang, J. (2013) Fabrication and reduction-sensitive behavior of polyion complex nano-micelles based on PEG-conjugated polymer containing disulfide bonds as a potential carrier of anti-tumor paclitaxel. *Colloids Surf., B: Biointerfaces 110*, 59−65.
(17) Wu, G., Fang, Y. Z., Yang, S., Lupton, J. R., and Turner, N. D. (2004) Glutathione metabolism and its implications for health. *J. Nutr. 134*, 489−492.
(18) Duan, K., Zhang, X., Tang, X., Yu, J., Liu, S., Wang, D., Li, Y., and Huang, J. (2010) Fabrication of cationic nanomicelle from chitosan-graft-polycaprolactone as the carrier of 7-ethyl-10-hydroxy-camptothecin. *Colloids Surf., B: Biointerfaces 76*, 475−482.
(19) Li, Y., Xiao, K., Luo, J., Xiao, W., Lee, J. S., Gonik, A. M., Kato, J., Dong, T. A., and Lam, K. S. (2011) Well-defined, reversible disulfide cross-linked micelles for on-demand paclitaxel delivery. *Biomaterials 32*, 6633−6645.
(20) Wang, H., Tang, L., Tu, C., Song, Z., Yin, Q., Yin, L., Zhang, Z., and Cheng, J. (2013) Redox-responsive, core-cross-linked micelles capable of on-demand, concurrent drug release and structure disassembly. *Biomacromolecules 14*, 3706−3712.
(21) Koo, A. N., Min, K. H., Lee, H. J., Lee, S. U., Kim, K., Kwon, I. C., Cho, S. H., Jeong, S. Y., and Lee, S. C. (2012) Tumor accumulation and antitumor efficacy of docetaxel-loaded core-shell-corona micelles with shell-specific redox-responsive cross-links. *Biomaterials 33*, 1489−1499.
(22) Lee, S. Y., Tyler, J. Y., Kim, S., Park, K., and Cheng, J. X. (2013) FRET imaging reveals different cellular entry routes of self-assembled and disulfide bonded polymeric micelles. *Mol. Pharmacol. 10*, 3497−3506.
(23) Lee, S. Y., Kim, S., Tyler, J. Y., Park, K., and Cheng, J. X. (2013) Blood-stable, tumor-adaptable disulfide bonded mPEG-(Cys)4-PDLLA micelles for chemotherapy. *Biomaterials 34*, 552−561.
(24) Zhang, M. Z., Ishii, A., Nishiyama, N., Matsumoto, S., Ishii, T., Yamasaki, Y., and Kataoka, K. (2009) PEGylated calcium phosphate nanocomposites as smart environment-sensitive carriers for siRNA delivery. *Adv. Mater. 21*, 3520−3525.
(25) Cabral, H., Matsumoto, Y., Mizuno, K., Chen, Q., Murakami, M., Kimura, M., Terada, Y., Kano, M. R., Miyazono, K., Uesaka, M., Nishiyama, N., and Kataoka, K. (2011) Accumulation of sub-100 nm polymeric micelles in poorly permeable tumours depends on size. *Nat. Nanotechnol. 6*, 815−823.
(26) Yokoyama, M. (1992) Block copolymers as drug carriers. *Crit. Rev. Ther. Drug Carrier Syst. 9*, 213−48.
(27) Huang, Y., Lu, J., Gao, X., Li, J., Zhao, W., Sun, M., Stolz, D. B., Venkataramanan, R., Rohan, L. C., and Li, S. (2012) PEG-derivatized embelin as a dual functional carrier for the delivery of paclitaxel. *Bioconjugate Chem. 23*, 1443−1451.
(28) Haklai, R., Elad-Sfadia, G., Egozi, Y., and Kloog, Y. (2008) Orally administered FTS (salirasib) inhibits human pancreatic tumor growth in nude mice. *Cancer Chemother. Pharmacol. 61*, 89−96.
(29) Zhao, M., He, P., Xu, L., Hidalgo, M., Laheru, D., and Rudek, M. A. (2008) Determination of salirasib (S-trans,trans-farnesylthiosalicylic acid) in human plasma using liquid chromatography-tandem mass spectrometry. *J. Chromatogr., B: Anal. Technol. Biomed. Life Sci. 869*, 142−145.